Received: 16 August 2019 | Accepted: 24 September 2019

DOI: 10.1111/gcbb.12657

ORIGINAL RESEARCH

GLOBAL CHANGE BIOLOGY BIOENERGY

WILEY

Mechanisms underlying limited soil carbon gains in perennial and cover-cropped bioenergy systems revealed by stable isotopes

Chenglong Ye[1,2] | **Steven J. Hall**[1]

[1]Department of Ecology, Evolution, and Organismal Biology, Iowa State University, Ames, IA, USA

[2]College of Resources and Environmental Sciences, Nanjing Agricultural University, Nanjing, People's Republic of China

Correspondence
Steven J. Hall, Department of Ecology, Evolution, and Organismal Biology, Iowa State University, Ames, IA 50011, USA.
Email: stevenjh@iastate.edu

Funding information
Iowa Nutrient Research Center; University of Iowa; NSF, Grant/Award Number: DEB-1457805

Abstract

Removal of biomass for bioenergy production may decrease soil organic carbon. While perennials or cover-cropped grains often have greater root production than annual grain crops, they variably impact soil carbon and underlying mechanisms remain unclear. We used high-frequency measurements of soil respiration and natural abundance carbon stable isotopes to differentiate respiration sources, pool sizes, and decomposition rate constants during a 10 month incubation of soils collected to 1 m depth from a 10 year old field experiment in Iowa, United States. Conversion of corn–soybean rotations to reconstructed prairies or addition of a rye cover crop to continuous corn significantly altered respiration sources and dynamics of fast- and slow-cycling carbon (turnover times of weeks to months–years, respectively), but had little effect on bulk soil carbon and several extractable pools (except in fertilized prairie). Both unfertilized and fertilized prairies increased slow-cycling carbon pools relative to annual crops, but only in 0–25 cm soil. Compared with fertilized prairie, the unfertilized prairie significantly increased decomposition rates of fast- and slow-cycling carbon pools in 0–25 cm soil, likely explaining the lack of significant bulk soil carbon accrual despite twofold greater root production. Carbon derived from C_4 plants decomposed faster than C_3-derived carbon across all depths and cropping systems and contributions of C_3-carbon to respiration increased with depth. Respiration of cover crop-derived carbon was greatest in 0–25 cm soil but comprised >25% of respiration below 25 cm, implying a disproportionate impact of the cover crop on deep soil metabolism. However, the cover crop also increased the decomposition rates of fast- and slow-cycling carbon pools and decreased their pool sizes across all depths relative to corn without a cover crop. Despite their notable environmental benefits, neither unfertilized perennials nor cover crops necessarily promote rapid soil carbon sequestration relative to conventional annual bioenergy systems because of concomitant increases in decomposition.

KEYWORDS

C_3 and C_4 plants, carbon sequestration, carbon stable isotopes, carbonate, cover crop, deep soil, no-till, reconstructed prairie, soil respiration

1 | INTRODUCTION

Potential environmental benefits of bioenergy cropping systems substantially depend on their impacts to soil biogeochemical processes, particularly those related to soil organic carbon (SOC) accumulation and retention of nutrients (Lemus & Lal, 2005; Robertson et al., 2017). Corn–soybean rotations and continuous corn remain the dominant biofuel cropping systems in the United States. However, the incorporation of cover crops and perennial vegetation into diversified bioenergy systems provides important opportunities for enhancing ecosystem services at the landscape scale (Liebman, Helmers, Schulte, & Chase, 2013; Schulte et al., 2017). Growing cover crops during shoulder seasons between grain crops provides additional biomass, especially roots, that may reduce impacts of biomass removal on SOC stocks while ameliorating nitrate leaching (Austin, Wickings, McDaniel, Robertson, & Grandy, 2017; Martinez-Feria, Dietzel, Liebman, Helmers, & Archontoulis, 2016; Ruis & Blanco-Canqui, 2017; Thapa, Mirsky, & Tully, 2018). Perennial systems may offer even larger opportunities for SOC accrual and nitrogen (N) retention, perhaps due to increased root productivity and soil aggregate formation (Anderson-Teixeira, Davis, Masters, & Delucia, 2009; Carvalho, Hudiburg, Franco, & DeLucia, 2017; Collins et al., 2010; Qin, Dunn, Kwon, Mueller, & Wander, 2016). Yet, impacts of diversified versus conventional bioenergy cropping systems on SOC dynamics and other aspects of soil metabolism often remain challenging to detect, and underlying mechanisms of carbon (C) cycle impacts are often elusive. Here, we asked whether high-frequency measurements of respiration and its C stable isotope composition ($\delta^{13}C$ values) under controlled laboratory conditions could reveal shifts in SOC inputs and metabolism among soil depth profiles from conventional and diversified bioenergy cropping systems.

Quantifying cropping system impacts on net changes in SOC can be challenging given high spatial heterogeneity and slow rates of change (Goidts, Wesemael, & Crucifix, 2009). Several studies showed that small increases in SOC stocks on perennial grasslands could not be detected statistically (Garten & Wullschleger, 1999; Zan, Fyles, Girouard, & Samson, 2001). Significant soil C accumulation in perennial cropping systems may also occur below surface horizons, where spatial heterogeneity may be particularly high (Follett, Vogel, Varvel, Mitchell, & Kimble, 2012; Rumpel & Kögel-Knabner, 2011). Impacts of cover crops have also often been difficult to detect, with reports of neutral, positive, or even negative effects on SOC stocks (Olson, Ebelhar, & Lang, 2010; Poeplau & Don, 2015).

Changes in C fluxes, rather than the pools that they influence, may be easier to detect. Measurements and kinetic modeling of soil carbon dioxide (CO_2) emissions (i.e., soil respiration) and its $\delta^{13}C$ values provide another way to assess SOC dynamics that is particularly responsive to modifications of the soil environment, such as changes in substrate quantity and quality (Collins et al., 2000, 2010; Paul, Harris, Collins, Schulthess, & Robertson, 1999). Soil respiration is derived from C sources with a wide range of mean turnover times, from days to months for plant residues and decomposition by-products to years to decades for SOC associated with minerals and aggregates (von Lützow et al., 2007; Zimmermann, Leifeld, Schmidt, Smith, & Fuhrer, 2007). Curve fitting of soil respiration data allows estimation of the sizes and turnover rates of these pools and potential differences among treatments (Collins et al., 2000; Reichstein, Bednorz, Broll, & Kätterer, 2000).

Cropping systems that differ in the abundances of plants with C_3 and C_4 photosynthetic pathways alter the $\delta^{13}C$ values of C pools and fluxes, yielding additional information on the sources and dynamics of SOC (Ehleringer, Buchmann, & Flanagan, 2000). Measurements of $\delta^{13}C$ of soil respiration provide information on the relative importance and turnover times of C_3 versus C_4 sources as well as the contributions of new versus old C sources following changes in cropping systems (Collins et al., 2000, 2010). Variation in $\delta^{13}C$ values may be especially useful for assessing contributions of C inputs from cover crops and newly established perennials. For example, C derived from the cover crop winter rye (*Secale cereale*), a C_3 plant, might be distinguished from background C sources (often a C_3–C_4 mixture derived from corn and soybean) by comparing $\delta^{13}C$ values from grain systems with and without the cover crop. Similarly, C derived from perennial vegetation with mixtures of C_3 and C_4 plants may also be distinguished by comparing $\delta^{13}C$ values relative to the background of corn- and soybean-derived C. In mixed C_3–C_4 grain crop and prairie ecosystems, aboveground biomass production is often dominated by C_4 plants (corn and warm-season grasses, respectively; Jarchow et al., 2015; Kordbacheh, Jarchow, English, & Liebman, 2019). However, the relative contributions of C_3 versus C_4 plants to bulk and actively cycling SOC pools have received little attention.

Here, we used samples from soil depth profiles (0–1 m) in a long-term field experiment containing six replicated cropping system treatments managed for bioenergy production (corn following soybean, soybean following corn, continuous corn, continuous corn with a winter rye cover crop, prairie, and fertilized prairie) to test the effects of diversified versus conventional bioenergy systems on soil metabolism. We sought to combine comprehensive measurements of C pools and soil respiration, along with their $\delta^{13}C$ values, to quantify impacts of these cropping systems on SOC dynamics. We used high-frequency (1–4 day intervals) automated measurements of soil CO_2 fluxes and $\delta^{13}C$ values via a tunable diode laser to provide increased sampling resolution relative to previous studies with similar objectives, which often relied on relatively sparse measurements of $\delta^{13}C$ over time

(Blagodatskaya, Yuyukina, Blagodatsky, & Kuzyakov, 2011; Collins et al., 2000).

The objectives of this study were to: (a) explore the impacts of diversified cropping systems on soil CO_2 fluxes and their $\delta^{13}C$ values, as compared with continuous corn and corn/soybean rotations; (b) characterize the sizes and turnover rates of fast- (days–months) and slow- (years–decades) cycling soil C pools under different cropping systems and at different depths; (c) determine the relative contributions of different C inputs (e.g., C_4 vs. C_3) as sources of soil respiration among cropping systems. We hypothesized that (a) soil CO_2 fluxes and $\delta^{13}C$ values vary among cropping systems even when C pools are indistinguishable; (b) prairie vegetation (perennial grasses/forbs) and a rye cover crop grown with continuous corn increase the size of fast- and slow-cycling SOC pools relative to annual crops in surface and subsurface soil; (c) C_4-C derived from corn and warm-season prairie grasses dominates C pools and respiration among all treatments and depths.

2 | MATERIALS AND METHODS

2.1 | Study site

The Comparison of Biofuel Systems (COBS) experiment is located in north-central Iowa, United States (41°55′N, 93°45′E). From 1951 to 2011, the mean annual temperature was 9.1°C, with mean monthly temperatures ranging from −7.4°C in January to 23.2°C in July. Mean annual precipitation is 850 mm, with about 70% falling between April and September (Jarchow et al., 2015). Soils were primarily Webster silty clay loam (fine-loamy, mixed, superactive, mesic Typic Endoaquoll) and Nicollet loam (fine-loamy, mixed, superactive, mesic Aquic Hapludoll). Prior to initiation of the experiment in 2008, the site was used for long-term corn (*Zea mays*) and soybean (*Glycine max*) production. There were six cropping treatments (Jarchow et al., 2015; Liebman et al., 2013): a corn–soybean rotation with annual grain removal where corn was the most recent crop (hereafter C2), a corn–soybean rotation with annual grain removal where soybean was the most recent crop (hereafter S2), continuous corn with annual grain and about 50% stover removal (hereafter CC), continuous corn with annual grain and about 50% stover removal, with winter rye used as a cover crop (hereafter CCW), multispecies prairie with annual aboveground biomass removal (hereafter Pr), and fertilized multispecies prairie with annual aboveground biomass removal (hereafter PrF). Both prairies were harvested at the end of each growing season after a hard frost, and were mowed to a height of 8–15 cm (Daigh et al., 2015). The initial species composition for both prairie treatments contained 31 species, including C_3 grasses (12%), C_4 grasses (56%), legumes (8%), and forbs (24%) by seed weight (Jarchow & Liebman, 2013). These treatments were arranged in a randomized block design with four replicates for a total of 24 plots. Each plot was 61 m × 27 m (0.16 ha). All treatments were managed without tillage. Fertilizer management was unique for each cropping system. All treatments received N fertilizer except for the unfertilized prairie treatment and the soybean phase of the corn–soybean rotation. Both the unfertilized and fertilized prairies received 78 kg P_2O_5/ha and 146 kg K_2O/ha in 2008. The unfertilized prairie received no fertilizers from 2009 onward, while the fertilized prairie received 84 kg N ha^{-1} $year^{-1}$ in the form of ammonium nitrate in 2009 and 2010 and urea ammonium nitrate in 2011 and thereafter. The fertilized prairie also received 126 kg P_2O_5/ha and 195 kg K_2O/ha in 2016, and 112 kg P_2O_5/ha, 224 kg K_2O/ha, and 28 kg S/ha in 2017 based on soil testing. All the corn treatments received a consistent rate of N fertilizer (urea ammonium nitrate) at the time of corn planting, but variable amounts of fertilizer were side-dressed into each corn treatment after emergence based on the results of a late-spring nitrate test. Thus, nitrogen addition in all the corn treatments ranged from 105 to 221 kg N ha^{-1} $year^{-1}$ (Jarchow et al., 2015; Kordbacheh et al., 2019).

2.2 | Soil sampling and analysis

In October 2017, one core (25 cm diameter) was collected to a depth of 100 cm in each of the four replicate plots of each treatment. The cores were divided into four depths: 0–25, 25–50, 50–75, and 75–100 cm, for a total of 96 samples (6 treatments × 4 depths × 4 replicates), which were stored field-moist at 4°C prior to further analyses. Subsamples were analyzed for soil pH in 0.01 M $CaCl_2$ (1:1 soil:solution). Soil ammonium (NH_4^+) and nitrate (NO_3^-) were extracted with 2 M potassium chloride and determined using microplate colorimetry (Doane & Horwáth, 2003). Subsamples were oven dried for 24 hr at 105°C to determine gravimetric water content. Air-dried and ground subsamples were used to determine SOC, total nitrogen (TN), $\delta^{13}C$, and $\delta^{15}N$ using an elemental analyzer (Costech) in line with the ThermoFinnigan DeltaPlus XL isotope ratio mass spectrometer at Iowa State University, Ames, IA, United States.

Air-dried subsamples were sequentially extracted with nanopure water, sodium sulfate (Na_2SO_4), and sodium dithionite to release soluble organic C, organic C associated with weak cation bridges, and chemically reducible iron mineral phases, respectively. For dissolved organic C and Na_2SO_4-extracted C measurements, 0.25 g subsamples were sequentially extracted by nanopure water and 0.5 M Na_2SO_4 in a 1:50 soil:solution mass ratio, shaken for 2 hr, and then centrifuged for 15 min at 10,000 g. Then, for dithionite-extracted C measurement, the subsamples were combined with 0.4 g sodium dithionite and 45 ml nanopure water, shaken for 16 hr, and then centrifuged for 15 min at 10,000 g. Concentrations and $\delta^{13}C$ values of

extracted C were measured by boiling acidified samples in persulfate solution within sealed vials filled with CO_2-free air (Huang & Hall, 2017). The CO_2 oxidized from extracted C and their $\delta^{13}C$ values were measured on a tunable diode laser absorption spectrometer (TGA200A; Campbell Scientific) by injection (Hall, Huang, & Hammel, 2017). Dithionite-extracted C was corrected for a reagent blank and $\delta^{13}C$ values were not reported due to blank $\delta^{13}C$ variability; reagent C blanks for the other samples were negligible.

Soil carbonate and its $\delta^{13}C$ values were measured by acidification following Huang and Hall (2018). In brief, air-dried and ground subsamples were added to 100 ml bottles capped with Teflon septa sealed with aluminum crimps, flushed with CO_2-free air, and 3 M HCl was injected to each capped bottle to convert carbonate to CO_2. The CO_2 concentration in the bottles and $\delta^{13}C$ of CO_2 were measured on the TGA200A analyzer by injection. The content of SOC was calculated by subtracting carbonate C from total soil C. We calculated $\delta^{13}C$ of SOC, corrected for carbonate content and $\delta^{13}C$, using a mixing model as described below. We note that the acidification protocol described above caused minimal loss of SOC as CO_2 (<0.02% of the total C pool) in soils collected near the field site which did not contain carbonate (pH < 6).

2.3 | Laboratory incubation

Laboratory incubations enabled metabolic comparisons among cropping system treatments and depth increments under constant moisture and temperature, although they are not strictly representative of field conditions. Soil (990 g equivalent dry weight) from each plot and depth increment was added to tenite butyrate tubes (6 cm diameter, 30 cm tall, sealed with plastic lids on the bottom) to achieve a bulk density of 1.45 g soil/cm^3, which was based on field measurements from the site (Bach & Hofmockel, 2016). These bulk density values were also consistent with the subsequent measurements of Ibrahim, Chua-Ona, Liebman, and Thompson (2018) in these plots. Soil moisture in each core was adjusted as necessary to 0.2 g H_2O/g soil, corresponding to a water-filled pore space of 0.64 m^3/m^3. Tubes were frozen at −20°C to simulate winter conditions, and then thawed at 23°C immediately prior to the incubation. Although winter air temperature often reaches −20°C at this site, deeper soils may remain considerably warmer. However, previous work showed that subsequent microbial activity in annually frozen agricultural soils was generally little affected by storage at −20°C (Stenberg et al., 1998). The tubes were sealed with plastic lids equipped with two stainless steel Swagelok fittings and tubing for automated headspace gas sampling using a dynamic chamber approach (e.g., Moyes, Gaines, Siegwolf, & Bowling, 2010). Briefly, each soil tube was flushed with air at a constant rate (50 ml/min), allowing quasi-steady-state accumulation of CO_2 derived from soil respiration in the tube headspace. The outlet was normally vented to the laboratory using a three-way valve. During sampling periods, outlet flow from a given soil tube was diverted through a manifold and routed to the TGA200A for measurement of CO_2 mole fraction and $\delta^{13}C$ (Huang & Hall, 2017). Each sample was measured for 120 s, discarding the transient first 30 s of each measurement. Three standard tanks traceable to the World Meteorological Organization primary standards (X2007 CO_2 scale) were measured for calibration between every 12 samples.

Respiration rate was calculated as follows: $\text{Flux} = \frac{(C_o - C_i) \times \text{Flow}}{\text{Mass}}$, where C_o and C_i are the mole fractions of CO_2 measured at the soil tube outlet and inlet, respectively. "Flow" is the volumetric flow of air through the core, and "Mass" is the dry soil mass equivalent in each soil core. The inlet CO_2 values were measured from blank cores (no soil present) at 20 min intervals. Variation in the inlet CO_2 mole fraction and $\delta^{13}C$ value was decreased by equilibrating fresh air from the building ventilation system in two sequential 200 L containers.

At the end of the incubation, soil from each tube was homogenized for additional measurements of inorganic N and carbonate as described above. Net N mineralization was calculated as the change in total inorganic N content between the start and the end of incubation. In order to determine if microbial activity affected carbonate release, a subset of soil samples with different carbonate contents were autoclaved twice (121°C, 30 min; with 2 days in between) to compare soil CO_2 fluxes and $\delta^{13}C$ values in the presence or absence of microbes and test for physical processes that might affect $\delta^{13}C$ values. These autoclaved samples were also frozen at −20°C, and then thawed at 23°C immediately prior to the CO_2 flux measurements.

2.4 | Data analysis

A two-source mixing model was used to calculate $\delta^{13}C$ values of SOC (Equation 1).

$$\delta^{13}C_{SOC} = \frac{\delta^{13}C_{total} \times C_{total} - \delta^{13}C_{carbonate} \times C_{carbonate}}{C_{total} - C_{carbonate}}. \quad (1)$$

Here, $\delta^{13}C_{SOC}$, $\delta^{13}C_{total}$, and $\delta^{13}C_{carbonate}$ denote the $\delta^{13}C$ values of SOC, total C, and carbonate, respectively; C_{total} and $C_{carbonate}$ denote the concentrations of total soil C and carbonate C, respectively.

The $\delta^{13}C$ of soil respiration from the soil tubes was similarly calculated using a mixing model that corrected the $\delta^{13}C$ and CO_2 mole fraction observed at the soil tube outlet ($\delta^{13}C_o$ and C_o, respectively) for the $\delta^{13}C$ value ($\delta^{13}C_i$) and CO_2 mole fraction (C_i) of the inlet air (Equation 2):

$$\delta^{13}C_{respiration} = \frac{\delta^{13}C_o \times C_o - \delta^{13}C_i \times C_i}{C_o - C_i}. \quad (2)$$

We used several additional mixing models to partition sources of soil respiration among different potential

end-members in each cropping system treatment. We assigned generic end-member values for C derived from C_3 and C_4 vegetation of −30‰ and −10‰, respectively. These values were selected to encompass the majority of observed variation in $\delta^{13}C$ values of soil respiration, and are consistent with extreme observed end-members of C_3 and C_4 leaf tissues (Cerling et al., 1997). The relatively high $\delta^{13}C$ value chosen for the C_4 end-member reflects the fact that roots and soil respiration are consistently offset from bulk leaf tissue $\delta^{13}C$ by ~2‰ (Bowling, Pataki, & Randerson, 2008), thus bounding observed variation in $\delta^{13}C$ values of CO_2. We note that using narrower end-member values for C_3 and C_4 plants has a small absolute effect on the calculated flux from each component, but results are qualitatively similar with the wider end-member values chosen here.

A two-source mixing model was used to estimate the fractional contribution of C_3- and C_4-derived C to respiration (Equations 3 and 4).

$$f_{C3} = \frac{\delta^{13}C_{\text{respiration}} - C_4}{C_3 - C_4}, \tag{3}$$

$$f_{C4} = 1 - f_{C3}. \tag{4}$$

Here, f_{C3} and f_{C4} are the fractions of respiration derived from C_3- and C_4-derived C, respectively. $\delta^{13}C_{\text{respiration}}$, C_3, and C_4 denote the $\delta^{13}C$ values of soil respiration, C_3, and C_4 vegetation, respectively.

To estimate the fractional contribution of the rye cover crop to respiration in the CCW treatment, we used a two-source mixing model incorporating the CC treatment as a control (Equation 5).

$$f_{\text{rye}} = \frac{\delta^{13}C_{\text{CCW}} - \delta^{13}C_{\text{CC}}}{\delta^{13}C_{\text{rye}} - \delta^{13}C_{\text{CC}}}. \tag{5}$$

Here, f_{rye} is the fraction of respiration derived from rye cover crop, and $\delta^{13}C_{\text{rye}}$, $\delta^{13}C_{\text{CCW}}$, and $\delta^{13}C_{\text{CC}}$ denote the $\delta^{13}C$ values of rye cover crop, respiration in the CCW, and CC treatments, respectively. We used −30‰ to estimate the $\delta^{13}C$ value of C derived from rye, a C_3 plant.

2.5 | Soil organic C mineralization kinetic models

The SOC mineralization kinetics were fit with a two-component exponential model (Equation 6; Reichstein et al., 2000).

$$C_{\text{min}}(t) = C_f \times \left(1 - e^{-k_f t}\right) + C_s \times \left(1 - e^{-k_s t}\right), \tag{6}$$

where $C_{\text{min}}(t)$ is the cumulative amount of carbon mineralized at time t (μg CO_2-C), C_f is the fast-decomposing C fraction (μg CO_2-C), and C_s is the slow-decomposing C fraction (μg CO_2-C). The first-order decomposition rate constants k_f and k_s (year^{-1}) correspond to the fast- and slow-decomposing fractions, respectively.

2.6 | Statistical analysis

A two-way ANOVA was used to assess the effects of treatment, soil depth, and their interactions on the response variables described above. Then, Tukey multiple comparison tests were used to test the effects of cropping system or soil depth on above biotic and abiotic properties, parameters of the two-component exponential model, and C mineralized from different sources.

We observed a brief period of very high $\delta^{13}C$ values of CO_2 early in the experiment (Figure S1c), consistent with release of inorganic C as CO_2 as a consequence of microbial activity and associated production of acidity due to processes such as nitrification (Figures S2 and S3). These high $\delta^{13}C$ values rapidly decreased over several days, and then stabilized or assumed a gradual decline (Figure S1c). In order to diminish potential effects of inorganic C (hereafter, referred to as carbonate) release as CO_2 on kinetic modeling and mixing model results, we used the piecewise.linear function in the "SiZer" package (Sonderegger, 2011) to perform a broken stick analysis to quantify the timepoint at which $\delta^{13}C$ values of soil respiration had approximately stabilized (17 days). We excluded CO_2 flux data before this point. However, we note that cumulative $\delta^{13}C$ values of soil respiration over the entire experiment were not significantly influenced by this 17 day period (Figure S2), and there were no significant changes in soil inorganic C before and after the incubation (Table S1).

Linear regressions were performed to analyze the relationship between the $\delta^{13}C$ values of soil extractable C and SOC and between the $\delta^{13}C$ values of soil-respired CO_2 and soil C pools. Statistically significant differences were accepted at $p < .05$. Mean values ± *SE* were reported throughout the text. The optimal number of pools in the exponential decay models fitted to CO_2 data was evaluated by comparing nested models using the Akaike information criterion. All statistical analyses were performed using R version 3.3.3.

3 | RESULTS

3.1 | Soil properties

All six cropping systems showed strong variation in soil properties with depth, but few differences were apparent among cropping systems at a given depth. Soil pH increased and the concentrations of SOC, TN, NO_3^--N, NH_4^+-N, and net N mineralization rate decreased with depth ($p < .05$; Table 1). The SOC/TN ratio also tended to decrease with depth, but the differences were not significant in any cropping system except for PrF (Table 1). The $\delta^{15}N$ values of TN were similar among cropping systems and showed little variation with depth (Table 1). The

TABLE 1 Soil attributes by cropping system and depth increment. Treatments included corn (C2) and soybean (S2) in the corn–soybean rotation, continuous corn (CC), continuous corn with a rye cover crop (CCW), unfertilized prairie (Pr), and fertilized prairie (PrF) cropping systems

Treatment	Depth (cm)	pH	SOC (mg/g)	TN (mg/g)	C:N	$\delta^{15}N_{TN}$	NO_3^--N (mg/kg)	NH_4^+-N (mg/kg)	Net N Min. ($\mu g\ kg^{-1}\ day^{-1}$)
C2	0–25	6.7 (0.2)^{aA}	20.0 (1.9)^{aA}	1.7 (0.1)^{aA}	12.0 (0.3)^{aA}	6.33 (0.3)^{aA}	5.8 (0.8)^{bcA}	0.35 (0.05)^{aA}	56.1 (24.4)^{aA}
	25–50	6.7 (0.3)^{aA}	11.8 (2.9)^{aAB}	0.9 (0.2)^{aB}	12.0 (0.8)^{aA}	6.74 (0.7)^{aA}	2.0 (0.4)^{bcB}	0.38 (0.06)^{aA}	1.3 (5.5)^{aB}
	50–75	6.9 (0.3)^{aA}	6.3 (1.9)^{aBC}	0.5 (0.1)^{aBC}	11.0 (1.4)^{aA}	6.84 (0.2)^{aA}	1.5 (0.3)^{aB}	0.32 (0.07)^{aA}	−4.2 (1.1)^{aB}
	75–100	7.3 (0.3)^{aA}	2.5 (1.2)^{aC}	0.3 (0.1)^{aC}	7.4 (2.1)^{aA}	6.11 (0.4)^{aA}	0.8 (0.1)^{aB}	0.22 (0.07)^{aA}	−1.8 (0.4)^{aB}
S2	0–25	7.1 (0.1)^{aA}	15.4 (4.1)^{aA}	1.3 (0.3)^{aA}	11.2 (0.4)^{aA}	7.04 (0.5)^{aA}	9.8 (1.5)^{cA}	0.31 (0.15)^{aA}	25.7 (6.3)^{aA}
	25–50	6.8 (0.3)^{aA}	10.2 (1.9)^{aAB}	0.9 (0.2)^{aA}	11.6 (0.4)^{aA}	7.09 (0.3)^{aA}	3.0 (0.3)^{cB}	0.22 (0.14)^{aA}	0.9 (3.5)^{aB}
	50–75	6.9 (0.3)^{aA}	6.1 (2.3)^{aBC}	0.6 (0.2)^{aA}	10.5 (1.0)^{aA}	6.67 (0.1)^{aAB}	2.2 (0.7)^{aB}	0.26 (0.07)^{aA}	4.0 (7.1)^{aB}
	75–100	7.2 (0.3)^{aA}	4.8 (3.4)^{aC}	0.4 (0.3)^{aA}	8.7 (1.3)^{aA}	5.72 (0.2)^{aB}	2.2 (1.0)^{aB}	0.17 (0.09)^{aA}	7.3 (8.7)^{aB}
CC	0–25	6.7 (0.1)^{aA}	18.9 (1.5)^{aA}	1.6 (0.1)^{aA}	12.0 (0.2)^{aA}	6.38 (0.3)^{aA}	5.4 (0.5)^{bA}	0.32 (0.04)^{aA}	52.0 (13.5)^{aA}
	25–50	6.6 (0.2)^{aA}	11.1 (2.2)^{aB}	0.9 (0.1)^{aB}	11.7 (0.8)^{aA}	7.04 (0.3)^{aA}	1.8 (0.2)^{abB}	0.39 (0.05)^{aA}	−3.1 (0.7)^{aB}
	50–75	7.2 (0.2)^{aAB}	4.7 (1.4)^{aBC}	0.5 (0.1)^{aBC}	9.0 (1.2)^{aA}	6.79 (0.4)^{aA}	1.6 (0.3)^{aB}	0.30 (0.05)^{aA}	−2.8 (1.3)^{aB}
	75–100	7.7 (0.0)^{aB}	2.5 (0.6)^{aC}	0.3 (0.0)^{aC}	10.1 (3.0)^{aA}	5.76 (0.6)^{aA}	0.8 (0.3)^{aB}	0.14 (0.05)^{aB}	−1.1 (1.1)^{aB}
CCW	0–25	6.5 (0.2)^{aA}	16.8 (2.2)^{aA}	1.4 (0.1)^{aA}	11.9 (0.5)^{aA}	6.59 (0.2)^{aA}	6.4 (1.2)^{bcA}	0.30 (0.06)^{aA}	56.2 (11.4)^{aA}
	25–50	6.4 (0.1)^{aA}	9.6 (2.2)^{aAB}	0.8 (0.1)^{aB}	12.2 (0.9)^{aA}	6.76 (0.4)^{aA}	1.7 (0.3)^{abB}	0.23 (0.07)^{aA}	−3.2 (0.3)^{aB}
	50–75	6.6 (0.1)^{aAB}	5.2 (1.6)^{aB}	0.5 (0.1)^{aB}	10.4 (1.0)^{aA}	6.49 (0.6)^{aA}	1.0 (0.2)^{aB}	0.27 (0.09)^{aA}	−1.8 (0.7)^{aB}
	75–100	7.1 (0.2)^{aB}	2.9 (1.0)^{aB}	0.3 (0.1)^{aB}	8.8 (1.1)^{aA}	5.58 (0.5)^{aA}	1.0 (0.3)^{aB}	0.20 (0.08)^{aA}	−2.4 (1.2)^{aB}
Pr	0–25	6.9 (0.2)^{aA}	17.2 (3.8)^{aA}	1.5 (0.3)^{aA}	11.3 (0.4)^{aA}	6.64 (0.5)^{aAB}	0.8 (0.1)^{aA}	0.49 (0.08)^{aA}	43.2 (10.9)^{aA}
	25–50	6.9 (0.3)^{aA}	9.1 (1.0)^{aAB}	0.8 (0.1)^{aAB}	11.6 (0.3)^{aA}	7.19 (0.3)^{aA}	0.7 (0.1)^{aA}	0.15 (0.06)^{aB}	−0.7 (0.6)^{aB}
	50–75	7.4 (0.2)^{aAB}	4.3 (0.8)^{aB}	0.3 (0.0)^{aC}	12.4 (1.6)^{aA}	6.68 (0.2)^{aA}	0.8 (0.4)^{aA}	0.11 (0.04)^{aB}	−1.6 (0.8)^{aB}
	75–100	7.8 (0.0)^{aB}	1.3 (0.5)^{aB}	0.1 (0.0)^{aC}	9.2 (2.8)^{aA}	4.93 (0.5)^{aB}	0.5 (0.2)^{aA}	0.06 (0.05)^{aB}	−0.9 (0.5)^{aB}
PrF	0–25	6.4 (0.2)^{aA}	24.3 (1.5)^{bA}	2.0 (0.1)^{aA}	12.2 (0.2)^{aA}	6.14 (0.3)^{aAB}	1.2 (0.7)^{aA}	0.60 (0.16)^{aA}	43.8 (8.6)^{aA}
	25–50	6.4 (0.3)^{aA}	11.4 (0.7)^{aB}	0.9 (0.1)^{aB}	12.2 (0.2)^{aA}	7.16 (0.4)^{aA}	0.7 (0.3)^{aA}	0.37 (0.08)^{aAB}	−1.1 (0.8)^{aB}
	50–75	7.1 (0.3)^{aAB}	4.6 (1.0)^{aC}	0.5 (0.1)^{aC}	9.3 (1.4)^{aB}	6.75 (0.3)^{aAB}	0.6 (0.1)^{aA}	0.37 (0.13)^{aAB}	−0.7 (0.4)^{aB}
	75–100	7.8 (0.0)^{aB}	3.6 (1.7)^{aC}	0.2 (0.0)^{aC}	9.4 (1.3)^{aB}	5.68 (0.4)^{aB}	0.6 (0.2)^{aA}	0.22 (0.07)^{aB}	−1.0 (1.1)^{aB}
	df	*F*	*F*	*F*	*F*	*F*	*F*	*F*	*F*
Treatment (*T*)	5	1.30^{NS}	1.08^{NS}	1.17^{NS}	0.06^{NS}	0.25^{NS}	21.96*	2.59**	0.13^{NS}
Depth (*D*)	3	7.80*	70.73*	94.56*	7.67*	13.00*	60.57*	7.52*	59.91*
$T \times D$	15	0.32^{NS}	0.69^{NS}	0.84^{NS}	0.53^{NS}	0.54^{NS}	6.08*	0.91^{NS}	0.91^{NS}

Note: Different lowercase letters denote significant differences among treatments at the same soil depth ($p < .05$). Different capital letters denote significant differences in the same treatment at different soil depths ($p < .05$). Values in parentheses are standard errors ($n = 4$).

Abbreviations: $\delta^{15}N_{TN}$, $\delta^{15}N$ of total nitrogen; *df*, degrees of freedom; *F*, variance ratio; Net N Min., net nitrogen mineralization rate; NS, no significance; SOC, soil organic carbon; TN, total nitrogen.

*$p < .01$;

**$p < .05$.

concentration of carbonate increased with depth in all cropping systems and its $\delta^{13}C$ values showed a tendency to decrease and then increase with depth (Table S1). No significant differences in carbonate concentration and its $\delta^{13}C$ values were observed before and after incubation (Table S1). The concentrations of dissolved organic C, Na_2SO_4-extracted C, and dithionite-extracted C, and the $\delta^{13}C$ values of SOC, dissolved organic C, and Na_2SO_4-extracted C significantly decreased with depth in all six cropping systems ($p < .05$; Tables 2 and 3), while cropping systems had little effect on the $\delta^{13}C$ values of these C pools (Table 3). Linear regressions showed that the $\delta^{13}C$ values of dissolved organic C and Na_2SO_4-extracted C were not significantly related to the $\delta^{13}C$ values of SOC (Figure S3).

Some of these soil properties varied among cropping systems at a given depth. In the surface soil (0–25 cm), PrF had significantly higher SOC concentration than the other five cropping systems and higher dissolved organic C than S2, respectively ($p < .05$; Tables 1 and 2). Across all soil depths, S2 tended to have higher NO_3^--N than the other five cropping systems, and significant differences were observed in 0–25 and 25–50 cm soil ($p < .05$; Table 1). In deeper soil (50–75 and 75–100 cm), S2 tended to have higher net N

TABLE 2 Extractable organic carbon in the deionized water (dissolved organic C), sodium sulfate (Na_2SO_4), and dithionite sequential extractions

Treatment	Depth (cm)	Dissolved organic C (mg/kg)	Na_2SO_4-extracted C (mg/kg)	Dithionite-extracted C (mg/kg)
C2	0–25	252 (30)^{abA}	228 (29)^{aA}	1,532 (198)^{aA}
	25–50	155 (43)^{aAB}	101 (9)^{aB}	1,207 (385)^{aA}
	50–75	97 (27)^{aB}	48 (4)^{aB}	793 (72)^{aA}
	75–100	54 (21)^{aB}	34 (9)^{aB}	1,263 (264)^{aA}
S2	0–25	183 (27)^{bA}	247 (29)^{aA}	1,479 (180)^{aA}
	25–50	150 (7)^{aA}	152 (11)^{aA}	1,147 (308)^{aA}
	50–75	94 (23)^{aB}	118 (65)^{aA}	1,081 (80)^{aA}
	75–100	99 (50)^{aB}	79 (49)^{aA}	915 (374)^{aA}
CC	0–25	253 (11)^{abA}	215 (19)^{aA}	1,465 (142)^{aA}
	25–50	154 (23)^{aB}	83 (17)^{aB}	1,268 (233)^{aA}
	50–75	83 (15)^{aC}	49 (16)^{aB}	1,342 (294)^{aA}
	75–100	49 (4)^{aC}	46 (5)^{aB}	1,305 (342)^{aA}
CCW	0–25	234 (24)^{abA}	178 (23)^{aA}	1,122 (190)^{aA}
	25–50	142 (24)^{aB}	78 (15)^{aB}	1,289 (209)^{aA}
	50–75	71 (12)^{aBC}	36 (9)^{aB}	992 (85)^{aA}
	75–100	45 (6)^{aC}	25 (2)^{aB}	1,058 (38)^{aA}
Pr	0–25	210 (3)^{abA}	246 (51)^{aA}	2,263 (589)^{aA}
	25–50	136 (21)^{aB}	123 (17)^{aAB}	1,248 (197)^{aA}
	50–75	69 (10)^{aC}	64 (18)^{aB}	1,006 (622)^{aA}
	75–100	39 (3)^{aC}	33 (8)^{aB}	605 (167)^{aA}
PrF	0–25	329 (46)^{aA}	242 (43)^{aA}	2,071 (122)^{aA}
	25–50	176 (27)^{aB}	101 (22)^{aB}	1,126 (133)^{aB}
	50–75	86 (12)^{aBC}	51 (4)^{aB}	1,122 (110)^{aB}
	75–100	50 (7)^{aC}	35 (9)^{aB}	722 (74)^{aB}
	df	*F*	*F*	*F*
Treatment (*T*)	5	1.91^{NS}	3.71*	0.55^{NS}
Depth (*D*)	3	75.75*	61.92*	9.50*
$T \times D$	15	1.34^{NS}	0.28^{NS}	1.24^{NS}

Note: Different lowercase letters denote significant differences among treatments at the same soil depth ($p < .05$). Different capital letters denote significant differences in the same treatment at different soil depths ($p < .05$). Values in parentheses are standard errors ($n = 4$).

Abbreviations: C2, corn; CC, continuous corn; CCW, continuous corn with a rye cover crop; *df*, degrees of freedom; *F*, variance ratio; NS, no significance; Pr, unfertilized prairie; PrF, fertilized prairie; S2, soybean.

*$p < .01$.

TABLE 3 The $\delta^{13}C$ values of soil organic C (SOC), dissolved organic C (DOC), and sodium sulfate (Na_2SO_4) extracted organic C

Treatment	Depth (cm)	$\delta^{13}C_{SOC}$ (‰)	$\delta^{13}C_{DOC}$ (‰)	$\delta^{13}C_{Na_2SO_4}$ (‰)
C2	0–25	−17.2 (0.3)^{aA}	−17.3 (0.7)^{aA}	−17.3 (0.4)^{aA}
	25–50	−17.2 (0.7)^{aA}	−17.3 (1.0)^{aA}	−17.2 (1.2)^{aA}
	50–75	−17.9 (0.5)^{aA}	−20.2 (1.1)^{aA}	−16.4 (2.5)^{aA}
	75–100	−22.0 (2.3)^{B}	−22.7 (1.5)^{aA}	−23.7 (2.8)^{aA}
S2	0–25	−16.9 (0.3)^{aA}	−16.3 (1.0)^{aA}	−16.7 (0.4)^{aA}
	25–50	−16.6 (0.3)^{aA}	−18.1 (1.1)^{aA}	−16.4 (1.5)^{aA}
	50–75	−16.3 (0.7)^{abA}	−18.4 (1.8)^{aA}	−18.8 (0.6)^{aA}
	75–100	−19.5 (2.1)^{A}	−21.5 (1.7)^{aA}	−17.8 (0.7)^{aA}
CC	0–25	−16.7 (0.1)^{aA}	−16.4 (0.4)^{aA}	−16.2 (0.3)^{aA}
	25–50	−16.4 (0.2)^{aA}	−16.8 (0.3)^{aAB}	−17.5 (1.5)^{aA}
	50–75	−16.4 (0.1)^{abA}	−19.7 (1.4)^{aAB}	−16.8 (2.2)^{aA}
	75–100	−18.1 (1.8)^{A}	−20.9 (1.4)^{aB}	−21.5 (1.1)^{aA}
CCW	0–25	−17.4 (0.5)^{aA}	−17.1 (0.1)^{aA}	−16.5 (0.5)^{aA}
	25–50	−17.3 (1.0)^{aA}	−17.9 (0.2)^{aA}	−15.6 (1.4)^{aA}
	50–75	−17.7 (0.7)^{aA}	−18.1 (2.0)^{aA}	−20.0 (N/A)
	75–100	−18.0 (1.2)^{A}	−19.2 (0.6)^{aA}	−19.7 (2.6)^{aA}
Pr	0–25	−16.6 (0.2)^{aA}	−17.2 (0.2)^{aA}	−16.4 (0.1)^{aA}
	25–50	−15.9 (0.5)^{aA}	−17.5 (0.8)^{aA}	−17.2 (1.2)^{aA}
	50–75	−14.8 (0.7)^{bA}	−19.5 (1.5)^{aAB}	−15.1 (1.4)^{aA}
	75–100	−17.9 (N/A)	−21.7 (0.5)^{aB}	−21.6 (1.4)^{aB}
PrF	0–25	−17.5 (0.3)^{aA}	−18.1 (0.4)^{aA}	−17.8 (0.6)^{aA}
	25–50	−16.7 (0.3)^{aA}	−17.2 (0.6)^{aA}	−15.9 (0.2)^{aA}
	50–75	−17.1 (0.1)^{abA}	−19.3 (0.9)^{aAB}	−17.3 (1.4)^{aA}
	75–100	−20.8 (N/A)	−21.4 (1.5)^{aB}	−22.7 (0.2)^{aA}
	df	*F*	*F*	*F*
Treatment (*T*)	5	0.95^{NS}	0.66^{NS}	1.24^{NS}
Depth (*D*)	3	1.24^{NS}	22.72*	5.04*
$T \times D$	15	1.24^{NS}	0.41^{NS}	1.31^{NS}

Note: Different lowercase letters denote significant differences among treatments at the same soil depth ($p < .05$). Different capital letters denote significant differences in the same treatment at different soil depths ($p < .05$). Values in parentheses are standard errors ($n = 4$).
Abbreviations: $\delta^{13}C_{SOC}$, $\delta^{13}C$ of soil organic carbon; $\delta^{13}C_{DOC}$, $\delta^{13}C$ of dissolved organic carbon; $\delta^{13}C_{Na2SO4}$, $\delta^{13}C$ of Na_2SO_4-extracted organic carbon; *df*, degrees of freedom; *F*, variance ratio; N/A, standard error could not be determined because some replicates were below detection after accounting for inorganic C; NS, no significance.
*$p < .01$.

mineralization rates than the other five cropping systems, but no significant differences were observed (Table 1).

3.2 | Soil respiration and its $\delta^{13}C$ values

Soil respiration rate from all cropping systems decreased with depth and decreased rapidly over time during the first 60 days of the experiment, and then decreased more slowly (Figure 1a). Soil respiration rate differed among cropping systems in surface soil (0–25 cm; Figure 1a), where Pr and PrF had significantly higher cumulative CO_2 production than the others ($p < .05$; Figure 1b). However, no significant differences in respiration rate and cumulative CO_2 production were observed among the other four cropping systems (Figure 1a,b). For the remaining three soil depths (>25 cm), respiration rate and cumulative CO_2 production were statistically similar among the six cropping systems (Figure 1a,b).

The $\delta^{13}C$ values of respired CO_2 varied over time and with depth. At the beginning of the incubation, the $\delta^{13}C$ values of respired CO_2 peaked from all six cropping

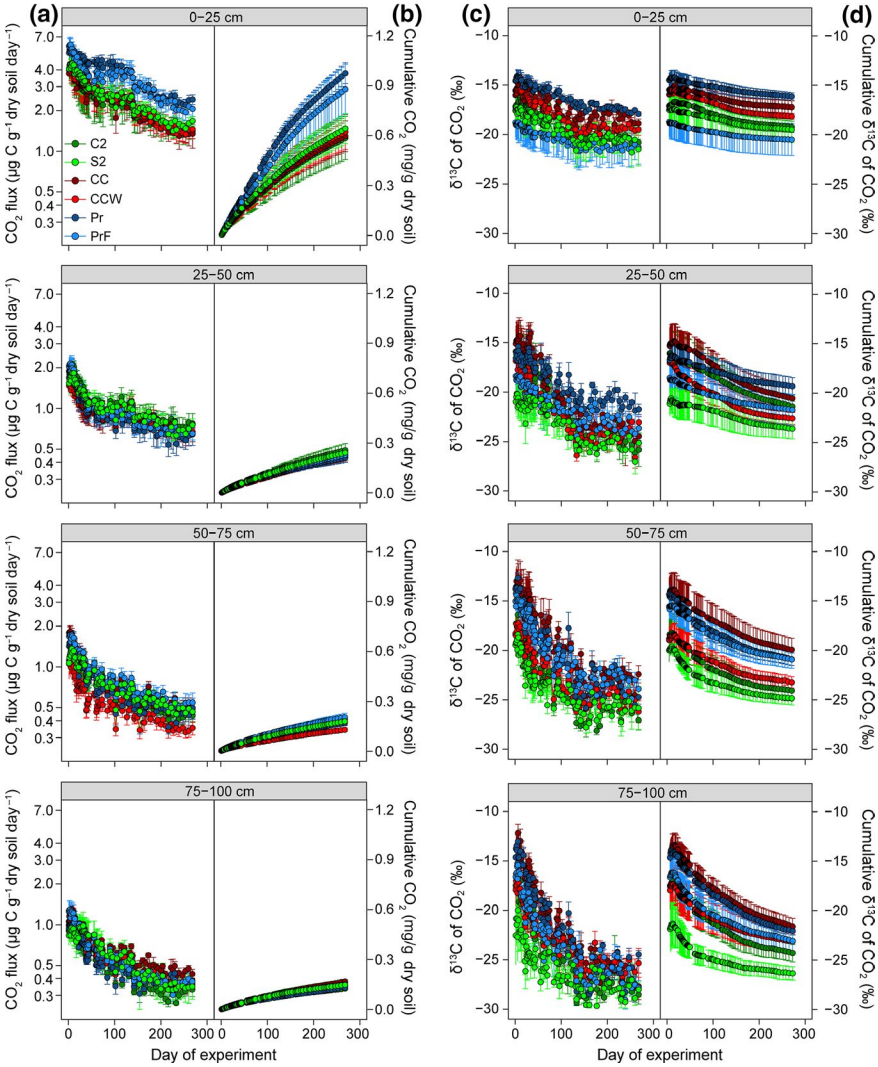

FIGURE 1 Soil respiration rate (a), cumulative respiration (b), $\delta^{13}C$ values of soil respiration (c), and cumulative $\delta^{13}C$ values of soil respiration (d) from corn (C2) and soybean (S2) in the corn–soybean rotation, continuous corn (CC), continuous corn with a rye cover crop (CCW), unfertilized prairie (Pr), and fertilized prairie (PrF) cropping systems (the first 17 days of data were removed)

systems across all soil depths and sharply declined over 17 days (Figure S1). After 17 days, the $\delta^{13}C$ values gradually declined over time (Figure 1c), and the post 17 day data were used for mixing model analyses. The $\delta^{13}C$ values of respired CO_2 tended to decrease with depth in all cropping systems and were more variable over time in deeper soil (Figure 1c). The $\delta^{13}C$ values of respired CO_2 also varied among cropping systems (Figure 1c). In 0–25 cm soil, Pr had the most positive $\delta^{13}C$ values of respired CO_2, followed by the CC, CCW, C2, and S2 cropping systems, and PrF had the lowest $\delta^{13}C$ values. Cumulative $\delta^{13}C$ values of respired CO_2 were significantly greater in Pr than in PrF ($p < .05$; Figure 1d). For soil below 25 cm, the $\delta^{13}C$ values of respired CO_2 tended to converge among the six cropping systems, but CC and Pr showed significantly more positive cumulative $\delta^{13}C$ values than S2 ($p < .05$; Figure 1c,d). Linear regressions showed that the $\delta^{13}C$ values of respired CO_2 were significantly related to the $\delta^{13}C$ values of SOC only in surface soil (0–25 cm; Figure S4), and were not related to the $\delta^{13}C$ values of dissolved organic C at any depth (Figure S5).

3.3 | Sources of mineralized C

For the surface soil (0–25 cm), PrF respired significantly more C_3-derived CO_2 than the other five cropping systems, while Pr respired significantly more C_4-derived CO_2 than the others, and no other significant differences were observed ($p < .05$; Figure 2a,b). For soil below 25 cm, cumulative mineralization of both C_3- and C_4-derived C was similar among cropping systems (Figure 2a,b). The proportions of CO_2 from C_3 and C_4 sources also varied among cropping systems and soil depths. In 0–25 cm soil, PrF respired the highest proportion of CO_2 from C_3-derived C (and thus the lowest C_4-derived C), followed by the S2, C2, CCW, and CC cropping systems, and Pr had the lowest proportion of CO_2 from C_3-derived C (and thus the highest C_4-derived C; Figure 2a,b). In soil below 25 cm, S2 respired the highest proportion of CO_2 from C_3-derived C (and thus, the lowest C_4-derived C), followed by the C2, CCW, PrF, and Pr cropping systems, and CC had the lowest proportion of CO_2 from C_3-derived C (and thus the highest C_4-derived C; Figure 2a,b). Respired CO_2 from the cover

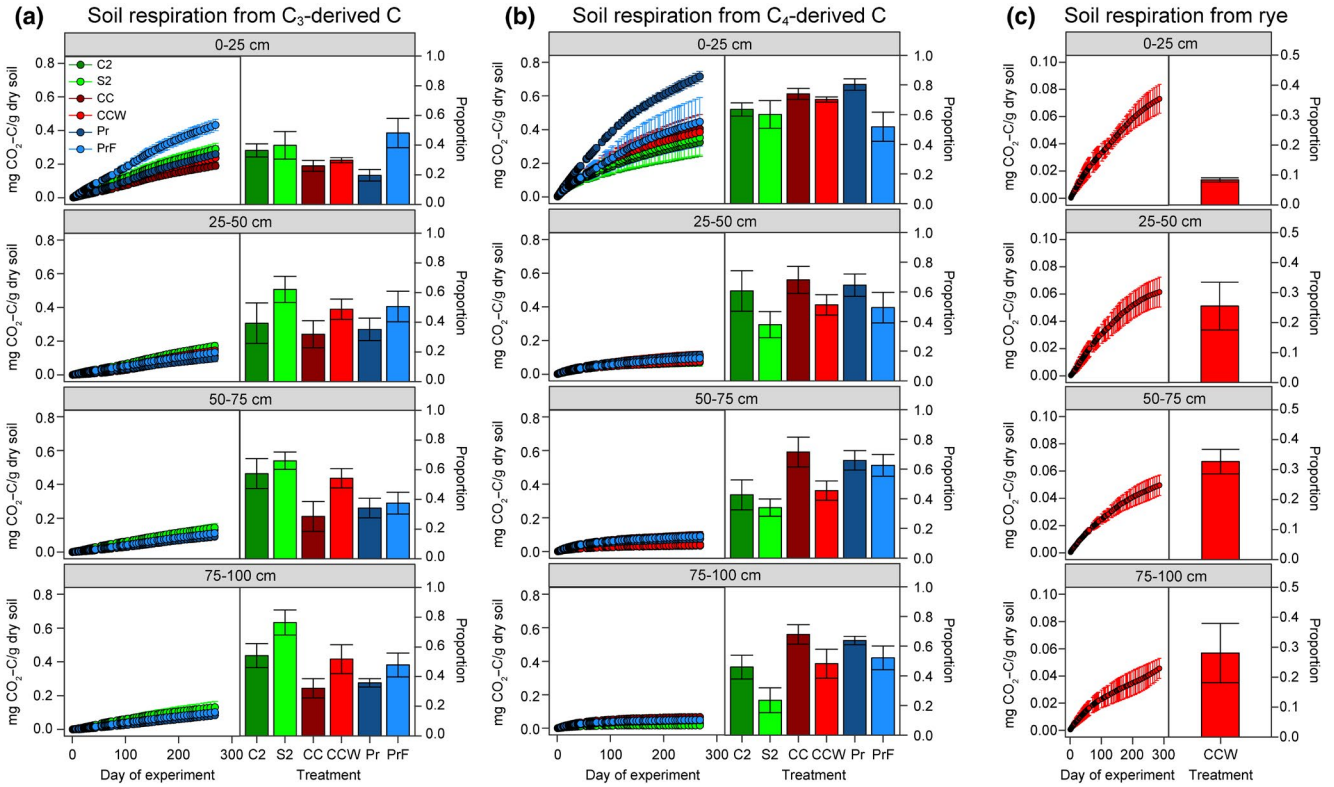

FIGURE 2 Cumulative respiration of C_3- (a) and C_4-derived C (b) and their proportion of total cumulative C mineralization from corn (C2) and soybean (S2) in the corn–soybean rotation, continuous corn (CC), continuous corn with a rye cover crop (CCW), unfertilized prairie (Pr), and fertilized prairie (PrF) cropping systems; cumulative mineralization of rye-derived C from continuous corn with a rye cover crop (CCW) system and its proportion of cumulative C mineralization (c)

crop significantly decreased, but its proportion of total respired CO_2 significantly increased with depth in CCW ($p < .05$; Figure 2c). Specifically, 0–25 cm soil had a lower proportion of cover crop-derived CO_2 (0.08 ± 0.007) than the other three depths (0.28 ± 0.08; Figure 2c).

3.4 | Soil C mineralization kinetics

A two-pool model was used to estimate fast- and slow-decomposing C (denoted by C_f and C_s, respectively) by fitting the cumulative CO_2 production curve for each incubated sample. The fitted models for all cropping systems closely approximated the data ($R^2 > .99$). The C_f pool represented 0.2%–1.1% of total SOC and had rate constants ranging from 8 to 126 year^{-1}, corresponding to mean turnover times ranging from 0.01 to 0.12 years (Table S2). The C_s pool represented 5%–21% of total SOC and had rate constants ranging from 0.5 to 1.6 year^{-1}, corresponding to mean turnover times ranging from 0.6 to 2.2 years (Table S2). The two prairies (Pr and PrF) had significantly higher amounts of C_s than all other treatments only in 0–25 cm soil ($p < .05$; Figure 3c). In contrast to the prairies, addition of a rye cover crop to continuous corn (CCW) did not increase C_f and C_s in 0–25 cm soil, and in soil below 25 cm, CCW had significantly lower amounts of C_s and C_f than CC while increasing their decomposition rates ($p < .05$; Figure 3).

The two-pool model was also used to estimate fast- and slow-decomposing pools of C_4-derived CO_2 (Figure S6), whereas C_3-derived CO_2 was best fit with a one-pool model (two-pool models did not converge during the model fitting process). For comparison, one-pool model parameters for C_3- and C_4-derived CO_2 are shown in Figure 4, and this single pool is hereafter termed the "active" C pool. The C_3-derived active pool represented 2%–20% of total SOC and had rate constants ranging from 0.2 to 0.7 year^{-1}, corresponding to mean turnover times ranging from 1.4 to 4.5 years (Table S3). The C_4-derived active pool represented 1%–6% of total SOC and had rate constants ranging from 1.5 to 5 year^{-1}, corresponding to mean turnover times ranging from 0.2 to 0.7 years (Table S3). Both C_3- and C_4-derived active pools significantly decreased with depth ($p < .05$; Figure 4a,c), while the decomposition rate constant of the C_4-derived active pool significantly increased with depth ($p < .05$; Figure 4d). In 0–25 cm soil, C2 and PrF had significantly larger C_3-derived active pools than S2 and Pr, respectively ($p < .05$; Figure 4a). The C2, CC, and PrF cropping systems had lower decomposition rate constants for the C_3-derived active pools than S2, CCW, and Pr, respectively (Figure 4b). The Pr and PrF cropping systems had significantly larger C_4-derived active pools but lower decomposition rate constants of these pools in 0–25 cm soil

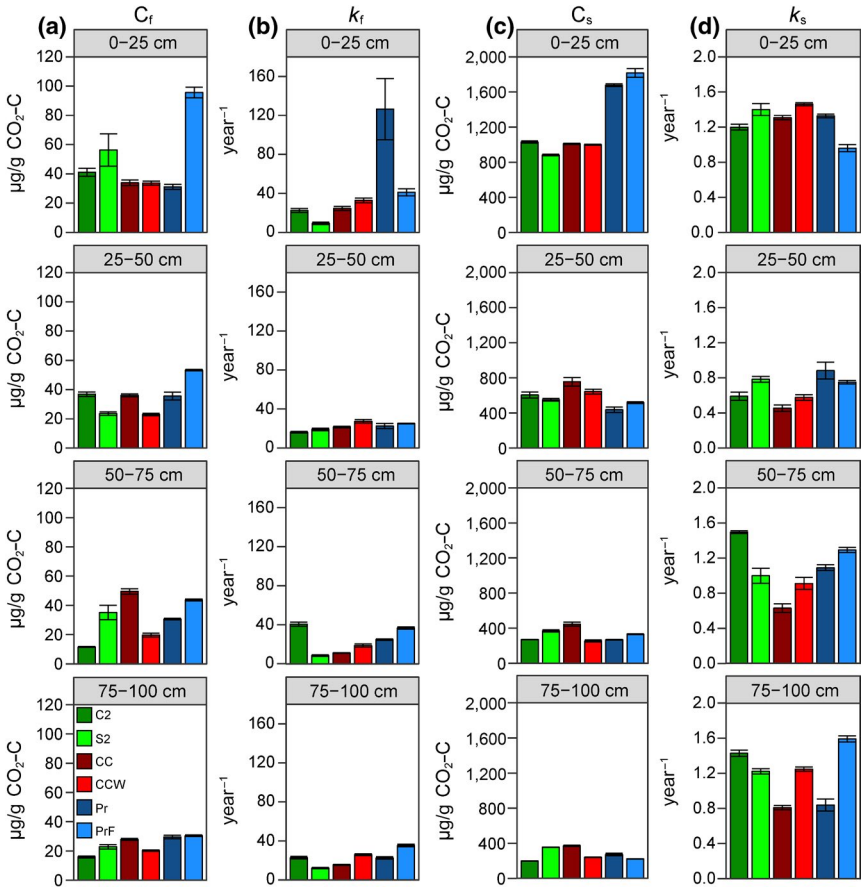

FIGURE 3 Parameters of the model used to fit the C mineralization kinetics: $CO_2\text{-}C(t) = C_f[1 - (\exp(-k_f t)] + C_s[1 - (\exp(-k_s t)]$. Constants are defined as follows: C_f, fast-decomposing C fraction (μg C/g) (a); k_f, first-order decomposition rate constant for the fast-decomposing fraction (year^{-1}) (b); C_s, slow-decomposing C fraction (μg C/g) (c); k_s, the first-order decomposition rate constant for the slow-decomposing fraction (year^{-1}) (d)

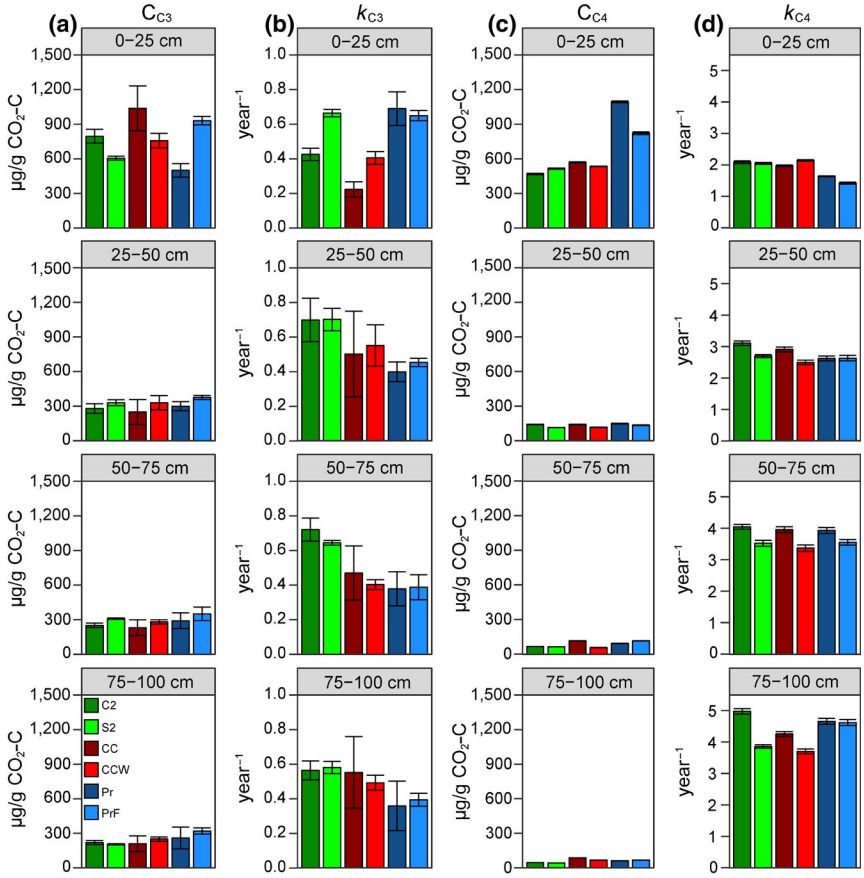

FIGURE 4 Parameters of the model used to fit the C mineralization kinetics: $CO_2\text{-}C(t) = C[1 - (\exp(-kt)]$. Constants are defined as follows: C_{C3}, C_3-derived C fraction (μg C/g) (a); k_{C3}, first-order decomposition rate constant for the C_3-derived fraction (year^{-1}) (b); C_{C4}, C_4-derived C fraction (μg C/g) (c); k_{C4}, the first-order decomposition rate constant for the C_4-derived fraction (year^{-1}) (d)

than the other four treatments ($p < .05$; Figure 4c,d). For soil below 25 cm, the C_3- and C_4-derived active pools did not significantly differ among cropping systems (Figure 4a,c). However, C2 and S2 had significantly higher decomposition rate constants for the C_3-derived active pool than Pr and PrF (Figure 4b) and C2 and CC had significantly higher decomposition rate constants for the C_4-derived active pool than S2 and CCW, respectively (Figure 4d).

3.5 | Autoclaved soil experiment

Autoclaving soil samples substantially reduced their CO_2 production relative to unaltered samples from the same plots and depth increments (Figure S7) while also decreasing their initial $\delta^{13}C$ values of CO_2 released from soil (Figure S8). As CO_2 production slowly increased over time in several of the autoclaved soils following microbial reestablishment, $\delta^{13}C$ tended to increase toward values observed in the control soils (Figure S8). There was no relationship between soil carbonate content and $\delta^{13}C$ of CO_2 or CO_2 flux in the autoclaved soils (Figure S8), implying that abiotic release of inorganic C was not significant.

4 | DISCUSSION

Soils from the bioenergy cropping systems examined here had few measurable differences in concentrations of total SOC and C released in several extraction solutions, even when sampled after 10 growing seasons (Tables 1 and 2). However, consistent with Hypothesis 1, they often significantly differed in the sources, fluxes, and turnover times of actively cycling C as reflected by soil respiration, its $\delta^{13}C$ values, and temporal trends in these fluxes quantified by kinetic modeling (Figures 1 and 3). Only partially supporting Hypotheses 2 and 3, the two prairies (fertilized and unfertilized) increased the size of the slow-cycling C pools relative to the grain cropping systems in 0–25 cm soil (Figure 3c), while addition of a rye cover crop to continuous corn decreased both fast- and slow-cycling C pools while increasing their decomposition rates in soil below 25 cm (Figure 3a,c). Regardless of cropping system, C_4-derived C consistently decomposed faster than C_3-derived C across all soil depths (Figure 4d). These results provide new insights on mechanisms by which diversified cropping systems may impact soil C cycling, which we discuss below.

4.1 | Contrasting impacts of unfertilized and fertilized prairie bioenergy systems on soil C cycling

Increases in SOC driven by prairie bioenergy crops have been largely attributed to organic C inputs from root biomass (Lemus & Lal, 2005), but the precise relationships among root productivity, soil C accrual, and treatments such as annual N fertilization remain unclear. Here, natural differences in C_4 versus C_3 plant dominance between Pr and PrF arising from plant community dynamics (Jarchow & Liebman, 2013; Kordbacheh et al., 2019) provided a unique opportunity to trace shifts in C cycling processes using stable isotopes. The relative increase of C_3 plants observed in the fertilized prairie is consistent with previous findings elsewhere and may be linked to the increased N requirement (i.e., lower C/N ratio and N-use efficiency) of C_3 versus C_4 plants (Wedin & Tilman, 1996). Averaged over the first 9 years of the study, the Pr treatment had 23% C_3 versus 77% C_4 cover, while PrF had 39% C_3 and 61% C_4 cover (Kordbacheh et al., 2019). This difference in plant cover was closely reflected in the $\delta^{13}C$ values of respiration in 0–25 cm soil, where C_3 contributions to CO_2 were estimated at 20% and 47% in Pr and PrF, respectively (Figure 2a). These differences in plant composition may impact longer term SOC dynamics, given that C_4-derived C apparently decomposed faster than C_3-derived C (Figure 4b,d). The phenomenon of intrinsically faster decomposition of C_4-derived C has been observed elsewhere (Wynn & Bird, 2007), although the underlying mechanism remains unknown.

The PrF treatment had significantly greater 0–25 cm SOC concentrations than the grain crop treatments whereas Pr did not (Table 1). This finding was surprising in that Pr had significantly greater root biomass than PrF, which was 2- and 1.5-fold greater between 0–20 and 20–100 cm, respectively (Dietzel, Liebman, & Archontoulis, 2017). The lack of a significant SOC increase in Pr as compared with PrF, despite increased root production in the former, was likely due to increased decomposition in Pr versus PrF soil. This interpretation is supported by 3- and 1.4-fold greater decomposition rate constants in the fast- and slow-cycling C pools of 0–25 cm soil in Pr than PrF (Figure 3b,d). In contrast, PrF had significantly larger fast- and slow-cycling C pools than Pr in 0–25 cm soil (Figure 3a,c). The larger C pool sizes and smaller decomposition rate constants in PrF inferred from the respiration data may have resulted from increased microbial C-use efficiency during decomposition or the suppression of microbial N mining from organic matter, which are often observed following N fertilization (Janssens et al., 2010; Manzoni, Taylor, Richter, Porporato, & Ågren, 2012; Yue et al., 2016). This rationale is consistent with previous measurements of greater microbial biomass in PrF (Bach & Hofmockel, 2015). Along with differences in the C_3- versus C_4-composition of plant inputs discussed above, these collective mechanisms likely contributed to increased bulk SOC concentrations in 0–25 cm PrF soil relative to Pr, despite the lower production of roots under N fertilization.

However, fast- and slow-cycling C pools did not consistently increase below 25 cm depth in either the Pr or PrF soils, nor were SOC concentrations affected. These findings are intriguing given that root production below 25 cm was significantly greater in Pr and PrF than in the other cropping

systems (Dietzel et al., 2017; Jarchow et al., 2015), but are consistent with other studies of perennial biofuel systems where soil C showed little change below the surface (Chimento, Almagro, & Amaducci, 2016; Qin et al., 2016; Richter, Agostini, Redmile-Gordon, White, & Goulding, 2015). Subsurface N limitation could contribute to the absence of increased soil respiration and transformation of roots to SOC in the prairies relative to the grain cropping systems below 25 cm depth: root biomass in Pr and PrF had greater C:N ratios than the annual crops (Dietzel et al., 2017), net N mineralization was consistently negative in soils below 25 cm during our incubation (Table 1), and fast- and slow-pool decomposition rate constants increased in response to N fertilization below 50 cm (Figure 3).

4.2 | Cover crops fueled soil respiration but decreased active C pool sizes in the subsoil

Contrary to Hypothesis 2, we found that inclusion of a rye cover crop with continuous corn did not increase fast- or slow-cycling C pool sizes nor bulk SOC relative to continuous corn without a cover crop (Table 1; Figure 3a,c). However, the cover crop increased the decomposition rate constants of fast- and slow-cycling C (Figure 3b,d). This is consistent with a microbial priming effect induced by cover crop residue inputs, whereby C inputs likely stimulated microbial growth and decomposition activity of extant C (Fontaine, Bardoux, Abbadie, & Mariotti, 2004), possibly a result of N limitation. As a consequence, decomposition rate constants increased in the presence of the cover crop, and below 25 cm depth, the sizes of both the fast- and slow-cycling C pools declined (Figure 3a,c). We suggest that previous reports of enhanced C and N cycling under cover crops (Hu et al., 1997; Sainju, Whitehead, & Singh, 2003) could also be linked in part to priming of organic matter decomposition.

In 0–25 cm soil, the cover crop accounted for ~9% of soil respiration (Figure 2c), consistent with previous estimates that the cover crop accounted for ~10% of corn stover aboveground residue C inputs (Martinez-Feria et al., 2016). However, the significant C cycling response to the cover crop in soil below 25 cm was intriguing given the narrow growth period for cover crops in Iowa (planting in October–November, dormancy during winter, and termination in May–June). Most previous studies have assessed biogeochemical impacts of cover crops in shallow soil (mean depth of 22 cm in the study of Poeplau & Don, 2015, but see Olson, Ebelhar, & Lang, 2014). At this site, observed increases in root biomass due to the cover crop (i.e., the difference in total root biomass between CCW and CC) were mostly confined to the top 30 cm (Jarchow et al., 2015). However, rye cover crop roots can extend to at least 50 cm (Sainju, Singh, & Whitehead, 1998), and previous sampling may not have detected the full extent of root production.

Irrespective of the absolute C inputs from the cover crop, the $\delta^{13}C$ data showed that they had a strong relative impact on soil metabolism, especially in the subsoil. The proportion of respired CO_2 derived from the cover crop increased below 25 cm, measuring almost 30% even in 75–100 cm soil (Figure 2c). In addition to subsoil root production, leaching of dissolved organic matter from cover crop surface residues or shallow roots likely contributed cover crop-derived C to the deeper soils. Winter rye is generally rich in soluble carbohydrates (Kuo, Sainju, & Jellum, 1997). In our study, winter rye was killed before corn planting in May/June, when precipitation is typically high in our region (Daigh et al., 2015; Jarchow et al., 2015). Thus, soluble or colloidal organic compounds produced during cover crop decomposition in surface soils could be transporated in percolating water along pore networks to the subsoil (Kaiser & Kalbitz, 2012), sustaining the significant soil respiration derived from cover crop C even at 1 m depth.

4.3 | Relationships among $\delta^{13}C$ values of C pools and fluxes

We found no systematic differences nor correlations between $\delta^{13}C$ values of dissolved organic C (DOC) and SOC (Table 3; Figure S3), in contrast to lower $\delta^{13}C$ values of DOC relative to SOC observed in some studies (Blagodatskaya et al., 2011; Coyle et al., 2009). We also found that the $\delta^{13}C$ values of CO_2 were initially higher than SOC and subsequently lower (Figure 1c; Table 3), consistent with preferential utilization of C_4-derived C and/or substrates such as carbohydrates that tend to have greater $\delta^{13}C$ values (Bowling et al., 2008; Wynn & Bird, 2007). However, cumulative respired CO_2 eventually had $\delta^{13}C$ values lower than SOC (by as much as several ‰) in almost all the cropping systems and depths (Figure S2), implying that bulk SOC was not isotopically representative of actively cycling pools in these mixed C_3–C_4 ecosystems. Linear regressions showed that the cumulative $\delta^{13}C$ values of CO_2 were only related to SOC in surface soil and were not related to DOC at any depth (Figures S4 and S5). Together, our data illustrate the utility of high-frequency $\delta^{13}C$ measurements of CO_2 for providing process-level insights that cannot necessarily be extrapolated from $\delta^{13}C$ values of C pools (Bowling et al., 2008).

4.4 | Faster decomposition of C_4- than C_3-derived C

We hypothesized that the larger biomass production from corn or prairie grasses relative to soybean or prairie forbs would make C_4-derived C the dominant source of soil respiration in these cropping systems. Indeed, in 0–25 cm soil, respiration from all cropping systems was dominated by C_4-derived C (Figure 2b), even where C_3 plants provided most of the recent

C inputs (i.e., S2 soil, which was most recently planted to soybean). However, this result was partly explained by the consistently faster decomposition rates of C_4- versus C_3-derived C (Figure 4). A similar finding of faster decomposition of C_4-derived C was observed across Australian soils with mixed C_3–C_4 vegetation (Wynn & Bird, 2007). The mechanisms underlying this phenomenon remains unclear, but could be linked to decreased microbial C-use efficiency accompanying the lower N content of C_4 plants, or anatomical or biochemical differences between C_3 and C_4 plant tissues.

In ecosystems dominated by C_3 vegetation, $\delta^{13}C$ values of SOC often increase slightly with depth due to several factors, such as greater contributions of $\delta^{13}C$-enriched microbial necromass to SOC and increasing $\delta^{13}C$ values of atmospheric CO_2 over time (Ehleringer et al., 2000). However, as depth increased, we observed stable or decreasing $\delta^{13}C$ values of all C pools and fluxes across soils from all cropping systems. These soils have received inputs of both C_3- and C_4-derived C during the course of their development under tallgrass prairie vegetation during the last 10,000 years (Wang, Cerling, & Effland, 1993), and during their last ~150 years of cultivation. Contrary to our third hypothesis, the trends toward decreasing $\delta^{13}C$ values of soil C and soil respiration with depth were consistent with the disproportionate persistence of C_3-derived C in actively cycling C and possibly in organic matter, given that C inputs in all soils would have likely have been dominated by C_4 biomass inputs for decades (if not centuries) before the experiment began. For example, corn is the dominant source of biomass in corn–soybean rotations (Russell, Cambardella, Laird, Jaynes, & Meek, 2009), and $\delta^{13}C$ values of pedogenic carbonates suggest that C_4 grasses dominated (75%) the biomass of pre-European-settlement prairies in our study region (Wang et al., 1993). Similar to our results, Li, McCarty, Karlen, Cambardella, and Effland (2018) found that mean C_4-derived C density was 31% lower than C_3-derived C in a field under long-term corn–soybean cultivation several km from our study site. Together, our data suggest that C derived from C_3 plants may persist disproportionately in soil—a factor that deserves further research attention and could influence management for soil C sequestration. Future examinations of SOC $\delta^{13}C$ values along soil depth profiles from mixed C_3–C_4 ecosystems could provide additional insights into the potential influence of plant photosynthetic pathways on SOC accrual.

4.5 | Patterns in inorganic C and its $\delta^{13}C$ values

We found that carbonate content increased strongly with depth and that trace amounts were present even in 0–25 cm soil (Table S1). Previous application of lime during farm management almost certainly contributed to the observed carbonate, especially at the surface. The trend of decreasing carbonate $\delta^{13}C$ values from the surface to the middle of the profile, increasing to more positive values at the bottom, may reflect a shift from agricultural lime to pedogenic carbonate to parent material carbonate, respectively. Overall, the range of carbonate $\delta^{13}C$ values we observed was consistent with other nearby soils under native prairie and alfalfa (Wang et al., 1993). Previous work at the COBS experiment interpreted total C in the subsoil as organic C (Dietzel et al., 2017). However, our data showed that accounting for the inorganic C content of these soils was critical, especially in the subsurface, where inorganic C was typically more than fivefold greater than organic C (Table S1).

The carbonate-derived CO_2 that was released early in the incubation experiment may have been formed during the soil freezing process we imposed immediately before the incubation, as freezing can promote new carbonate formation (Cerling, 1984). Overall, however, microbial carbonate release was not detectable as a change in soil carbonate stocks and had no significant net effect on $\delta^{13}C$ of cumulative C mineralization (Figure S2; Table S1). Thus, our results indicated little effect of soil carbonate on soil respiration and its $\delta^{13}C$ values except for the initial stage of incubation.

4.6 | Implications for bioenergy cropping system C dynamics

Partial conversion of annual grain crops to perennial vegetation, or the addition of cover crops to grain cropping systems, has the potential to partially offset negative ecological effects of residue removal for bioenergy production (Ruis & Blanco-Canqui, 2017; Tiemann & Grandy, 2015). However, although these measures can provide additional plant biomass, they do not necessarily lead to measurable increases in SOC storage over timescales of years to decades (Kuo et al., 1997; Poeplau & Don, 2014, 2015; Zan et al., 2001), including the study site we examined here (Ibrahim et al., 2018). Based on our results, several biogeochemical mechanisms may explain this finding, beyond the simple fact that changes in soil C stocks are difficult to detect. First, biomass produced from the prairie cropping system decomposed more quickly in the absence of N fertilization, presumably due to increased microbial N mining from organic matter, decreased microbial C-use efficiency, and/or the increased dominance of C_4 vegetation. This meant that accrual of soil C was lower in Pr soil than PrF, despite having twofold greater root productivity, and its soil C concentrations were not statistically different from any of the grain cropping systems. This finding suggests that N limitation may be an important constraint on SOC accrual in reconstructed prairie bioenergy systems via both direct and indirect mechanisms, even where root production is high.

Second, inclusion of a rye cover crop enhanced decomposition rates throughout the soil profile but did not increase C pool sizes. This response may have been linked to priming and/or N limitation which stimulated decomposition of extant soil C. Previous work at COBS indicated higher N fertilization requirements for CCW than CC, and significant attenuation of nitrate leaching in the former treatment (Martinez-Feria et al., 2016). Our results suggest that stimulation of microbial metabolism throughout the soil profile may contribute to increased N retention under a rye cover crop. However, for the same reason that cover crops are effective at stimulating N immobilization, they may also lead to increased decomposition rates, at least partially offsetting opportunities for C accrual. Although perennial vegetation and cover crops have critical environmental benefits, especially with regard to nutrient retention, we urge caution in assuming that increased belowground plant productivity necessarily leads to SOC accrual in cropping systems managed for bioenergy production. These findings are particularly relevant in the context of ambitious efforts to promote SOC sequestration as a key element of global climate policy (Minasny et al., 2017), where low-fertility perennial and cover-cropped grain systems would presumably play key roles.

ACKNOWLEDGEMENTS

This study was supported in part by the Center for Global and Regional Environmental Research at the University of Iowa and the Iowa Nutrient Research Center, and C isotope analysis methods were developed with support from NSF grant DEB-1457805. We thank Matt Liebman for facilitating access to the study site and for thoughtful comments, Wenjuan Huang for assistance with data analysis, and two anonymous reviewers.

ORCID

Steven J. Hall https://orcid.org/0000-0002-7841-2019

REFERENCES

Anderson-Teixeira, K. J., Davis, S. C., Masters, M. D., & Delucia, E. H. (2009). Changes in soil organic carbon under biofuel crops. *Global Change Biology – Bioenergy*, *1*, 75–96. https://doi.org/10.1111/j.1757-1707.2008.01001.x

Austin, E. E., Wickings, K., McDaniel, M. D., Robertson, G. P., & Grandy, A. S. (2017). Cover crop root contributions to soil carbon in a no-till corn bioenergy cropping system. *Global Change Biology – Bioenergy*, *9*, 1252–1263. https://doi.org/10.1111/gcbb.12428

Bach, E. M., & Hofmockel, K. S. (2015). Coupled carbon and nitrogen inputs increase microbial biomass and activity in prairie bioenergy systems. *Ecosystems*, *18*, 417–427. https://doi.org/10.1007/s10021-014-9835-8

Bach, E. M., & Hofmockel, K. S. (2016). A time for every season: Soil aggregate turnover stimulates decomposition and reduces carbon loss in grasslands managed for bioenergy. *Global Change Biology – Bioenergy*, *8*, 588–599. https://doi.org/10.1111/gcbb.12267

Blagodatskaya, E., Yuyukina, T., Blagodatsky, S., & Kuzyakov, Y. (2011). Turnover of soil organic matter and of microbial biomass under C3–C4 vegetation change: Consideration of ^{13}C fractionation and preferential substrate utilization. *Soil Biology and Biochemistry*, *43*, 159–166. https://doi.org/10.1016/j.soilbio.2010.09.028

Bowling, D. R., Pataki, D. E., & Randerson, J. T. (2008). Carbon isotopes in terrestrial ecosystem pools and CO_2 fluxes. *New Phytologist*, *178*, 24–40. https://doi.org/10.1111/j.1469-8137.2007.02342.x

Carvalho, J. L., Hudiburg, T. W., Franco, H. C., & DeLucia, E. H. (2017). Contribution of above-and belowground bioenergy crop residues to soil carbon. *Global Change Biology – Bioenergy*, *9*, 1333–1343. https://doi.org/10.1111/gcbb.12411

Cerling, T. E. (1984). The stable isotopic composition of modern soil carbonate and its relationship to climate. *Earth and Planetary Science Letters*, *71*, 229–240. https://doi.org/10.1016/0012-821X(84)90089-X

Cerling, T. E., Harris, J. M., MacFadden, B. J., Leakey, M. G., Quade, J., Eisenmann, V., & Ehleringer, J. R. (1997). Global vegetation change through the Miocene/Pliocene boundary. *Nature*, *389*, 153–158. https://doi.org/10.1038/38229

Chimento, C., Almagro, M., & Amaducci, S. (2016). Carbon sequestration potential in perennial bioenergy crops: The importance of organic matter inputs and its physical protection. *Global Change Biology – Bioenergy*, *8*, 111–121. https://doi.org/10.1111/gcbb.12232

Collins, H. P., Elliott, E. T., Paustian, K., Bundy, L. G., Dick, W. A., Huggins, D. R., … Paul, E. A. (2000). Soil carbon pools and fluxes in long-term corn belt agroecosystems. *Soil Biology and Biochemistry*, *32*, 157–168. https://doi.org/10.1016/S0038-0717(99)00136-4

Collins, H. P., Smith, J. L., Fransen, S., Alva, A. K., Kruger, C. E., & Granatstein, D. M. (2010). Carbon sequestration under irrigated switchgrass (*Panicum virgatum* L.) production. *Soil Science Society of America Journal*, *74*, 2049–2058. https://doi.org/10.2136/sssaj2010.0020

Coyle, J. S., Dijkstra, P., Doucett, R. R., Schwartz, E., Hart, S. C., & Hungate, B. A. (2009). Relationships between C and N availability, substrate age, and natural abundance ^{13}C and ^{15}N signatures of soil microbial biomass in a semiarid climate. *Soil Biology and Biochemistry*, *41*, 1605–1611. https://doi.org/10.1016/j.soilbio.2009.04.022

Daigh, A. L. M., Zhou, X., Helmers, M. J., Pederson, C. H., Horton, R., Jarchow, M., & Liebman, M. (2015). Subsurface drainage nitrate and total reactive phosphorus losses in bioenergy-based prairies and corn systems. *Journal of Environmental Quality*, *44*, 1638–1646. https://doi.org/10.2134/jeq2015.02.0080

Dietzel, R., Liebman, M., & Archontoulis, S. (2017). A deeper look at the relationship between root carbon pools and the vertical distribution of the soil carbon pool. *Soil*, *3*, 139–152. https://doi.org/10.5194/soil-3-139-2017

Doane, T. A., & Horwáth, W. R. (2003). Spectrophotometric determination of nitrate with a single reagent. *Analytical Letters*, *36*, 2713–2722. https://doi.org/10.1081/AL-120024647

Ehleringer, J. R., Buchmann, N., & Flanagan, L. B. (2000). Carbon isotope ratios in belowground carbon cycle processes. *Ecological Applications*, *10*, 412–422. https://doi.org/10.1890/1051-0761(2000)010[0412:CIRIBC]2.0.CO;2

Follett, R. F., Vogel, K. P., Varvel, G. E., Mitchell, R. B., & Kimble, J. (2012). Soil carbon sequestration by switchgrass and no-till maize grown for bioenergy. *BioEnergy Research*, *5*, 866–875. https://doi.org/10.1007/s12155-012-9198-y

Fontaine, S., Bardoux, G., Abbadie, L., & Mariotti, A. (2004). Carbon input to soil may decrease soil carbon content. *Ecology Letters*, *7*, 314–320. https://doi.org/10.1111/j.1461-0248.2004.00579.x

Garten, C. T., & Wullschleger, S. D. (1999). Soil carbon inventories under a bioenergy crop (switchgrass): Measurement limitations. *Journal of Environmental Quality*, *28*, 1359–1365. https://doi.org/10.2134/jeq1999.00472425002800040041x

Goidts, E., Van Wesemael, B., & Crucifix, M. (2009). Magnitude and sources of uncertainties in soil organic carbon (SOC) stock assessments at various scales. *European Journal of Soil Science*, *60*, 723–739. https://doi.org/10.1111/j.1365-2389.2009.01157.x

Hall, S. J., Huang, W., & Hammel, K. E. (2017). An optical method for carbon dioxide isotopes and mole fractions in small gas samples: Tracing microbial respiration from soil, litter, and lignin. *Rapid Communications in Mass Spectrometry*, *31*, 1938–1946. https://doi.org/10.1002/rcm.7973

Hu, S., Grunwald, N. J., Van Bruggen, A. H. C., Gamble, G. R., Drinkwater, L. E., Shennan, C., & Demment, M. W. (1997). Short-term effects of cover crop incorporation on soil carbon pools and nitrogen availability. *Soil Science Society of America Journal*, *61*, 901–911. https://doi.org/10.2136/sssaj1997.03615995006100030027x

Huang, W., & Hall, S. J. (2017). Elevated moisture stimulates carbon loss from mineral soils by releasing protected organic matter. *Nature Communications*, *8*, 1774. https://doi.org/10.1038/s41467-017-01998-z

Huang, W., & Hall, S. J. (2018). Large impacts of small methane fluxes on carbon isotope values of soil respiration. *Soil Biology and Biochemistry*, *124*, 126–133. https://doi.org/10.1016/j.soilbio.2018.06.003

Ibrahim, M. A., Chua-Ona, T., Liebman, M., & Thompson, M. L. (2018). Soil organic carbon storage under biofuel cropping systems in a humid, continental climate. *Agronomy Journal*, *110*(5), 1748. https://doi.org/10.2134/agronj2018.03.0204

Janssens, I. A., Dieleman, W., Luyssaert, S., Subke, J. A., Reichstein, M., Ceulemans, R., … Law, B. E. (2010). Reduction of forest soil respiration in response to nitrogen deposition. *Nature Geoscience*, *3*, 315–322. https://doi.org/10.1038/ngeo844

Jarchow, M. E., & Liebman, M. (2013). Nitrogen fertilization increases diversity and productivity of prairie communities used for bioenergy. *Global Change Biology – Bioenergy*, *5*, 281–289. https://doi.org/10.1111/j.1757-1707.2012.01186.x

Jarchow, M. E., Liebman, M., Dhungel, S., Dietzel, R., Sundberg, D., Anex, R. P., … Chua, T. (2015). Trade-offs among agronomic, energetic, and environmental performance characteristics of corn and prairie bioenergy cropping systems. *Global Change Biology – Bioenergy*, *7*, 57–71. https://doi.org/10.1111/gcbb.12096

Kaiser, K., & Kalbitz, K. (2012). Cycling downwards – Dissolved organic matter in soils. *Soil Biology and Biochemistry*, *52*, 29–32. https://doi.org/10.1016/j.soilbio.2012.04.002

Kordbacheh, F., Jarchow, M., English, L., & Liebman, M. (2019). Productivity and diversity of annually harvested reconstructed prairie communities. *Journal of Applied Ecology*, *56*, 330–342. https://doi.org/10.1111/1365-2664.13267

Kuo, S., Sainju, U. M., & Jellum, E. J. (1997). Winter cover crop effects on soil organic carbon and carbohydrate in soil. *Soil Science Society of America Journal*, *61*, 145–152. https://doi.org/10.2136/sssaj1997.03615995006100010022x

Lemus, R., & Lal, R. (2005). Bioenergy crops and carbon sequestration. *Critical Reviews in Plant Sciences*, *24*, 1–21. https://doi.org/10.1080/07352680590910393

Li, X., McCarty, G. W., Karlen, D. L., Cambardella, C. A., & Effland, W. (2018). Soil organic carbon and isotope composition response to topography and erosion in Iowa. *Journal of Geophysical Research: Biogeosciences*, *123*, 3649–3667. https://doi.org/10.1029/2018JG004824

Liebman, M., Helmers, M. J., Schulte, L. A., & Chase, C. A. (2013). Using biodiversity to link agricultural productivity with environmental quality: Results from three field experiments in Iowa. *Renewable Agriculture and Food Systems*, *28*, 115–128. https://doi.org/10.1017/S1742170512000300

Manzoni, S., Taylor, P., Richter, A., Porporato, A., & Ågren, G. I. (2012). Environmental and stoichiometric controls on microbial carbon-use efficiency in soils. *New Phytologist*, *196*, 79–91. https://doi.org/10.1111/j.1469-8137.2012.04225.x

Martinez-Feria, R. A., Dietzel, R., Liebman, M., Helmers, M. J., & Archontoulis, S. V. (2016). Rye cover crop effects on maize: A system-level analysis. *Field Crops Research*, *196*, 145–159. https://doi.org/10.1016/j.fcr.2016.06.016

Minasny, B., Malone, B. P., McBratney, A. B., Angers, D. A., Arrouays, D., Chambers, A., … Winowiecki, L. (2017). Soil carbon 4 per mille. *Geoderma*, *292*, 59–86. https://doi.org/10.1016/j.geoderma.2017.01.002

Moyes, A. B., Gaines, S. J., Siegwolf, R. T. W., & Bowling, D. R. (2010). Diffusive fractionation complicates isotopic partitioning of autotrophic and heterotrophic sources of soil respiration. *Plant, Cell & Environment*, *33*, 1804–1819. https://doi.org/10.1111/j.1365-3040.2010.02185.x

Olson, K. R., Ebelhar, S. A., & Lang, J. M. (2010). Cover crop effects on crop yields and soil organic carbon content. *Soil Science*, *175*, 89–98. https://doi.org/10.1097/SS.0b013e3181cf7959

Olson, K., Ebelhar, S. A., & Lang, J. M. (2014). Long-term effects of cover crops on crop yields, soil organic carbon stocks and sequestration. *Open Journal of Soil Science*, *4*, 284–292. https://doi.org/10.4236/ojss.2014.48030

Paul, E. A., Harris, D., Collins, H. P., Schulthess, U., & Robertson, G. P. (1999). Evolution of CO_2 and soil carbon dynamics in biologically managed, row-crop agroecosystems. *Applied Soil Ecology*, *11*, 53–65. https://doi.org/10.1016/S0929-1393(98)00130-9

Poeplau, C., & Don, A. (2014). Soil carbon changes under Miscanthus driven by C_4 accumulation and C_3 decompostion – Toward a default sequestration function. *Global Change Biology – Bioenergy*, *6*, 327–338. https://doi.org/10.1111/gcbb.12043

Poeplau, C., & Don, A. (2015). Carbon sequestration in agricultural soils via cultivation of cover crops – A meta-analysis. *Agriculture, Ecosystems & Environment*, *200*, 33–41. https://doi.org/10.1016/j.agee.2014.10.024

Qin, Z., Dunn, J. B., Kwon, H., Mueller, S., & Wander, M. M. (2016). Soil carbon sequestration and land use change associated with biofuel production: Empirical evidence. *Global Change Biology – Bioenergy*, *8*, 66–80. https://doi.org/10.1111/gcbb.12237

Reichstein, M., Bednorz, F., Broll, G., & Kätterer, T. (2000). Temperature dependence of carbon mineralisation: Conclusions from a long-term incubation of subalpine soil samples. *Soil Biology and Biochemistry*, *32*, 947–958. https://doi.org/10.1016/S0038-0717(00)00002-X

Richter, G. M., Agostini, F., Redmile-Gordon, M., White, R., & Goulding, K. W. (2015). Sequestration of C in soils under Miscanthus can be marginal and is affected by genotype-specific root distribution. *Agriculture, Ecosystems & Environment*, *200*, 169–177. https://doi.org/10.1016/j.agee.2014.11.011

Robertson, G. P., Hamilton, S. K., Barham, B. L., Dale, B. E., Izaurralde, R. C., Jackson, R. D., … Tiedje, J. M. (2017). Cellulosic biofuel contributions to a sustainable energy future: Choices and outcomes. *Science*, *356*(6345), eaal2324. https://doi.org/10.1126/science.aal2324

Ruis, S. J., & Blanco-Canqui, H. (2017). Cover crops could offset crop residue removal effects on soil carbon and other properties: A review. *Agronomy Journal*, *109*, 1785–1805. https://doi.org/10.2134/agronj2016.12.0735

Rumpel, C., & Kögel-Knabner, I. (2011). Deep soil organic matter – A key but poorly understood component of terrestrial C cycle. *Plant and Soil*, *338*, 143–158. https://doi.org/10.1007/s11104-010-0391-5

Russell, A. E., Cambardella, C. A., Laird, D. A., Jaynes, D. B., & Meek, D. W. (2009). Nitrogen fertilizer effects on soil carbon balances in Midwestern US agricultural systems. *Ecological Applications*, *19*, 1102–1113. https://doi.org/10.1890/07-1919.1

Sainju, U. M., Singh, B. P., & Whitehead, W. F. (1998). Cover crop root distribution and its effects on soil nitrogen cycling. *Agronomy Journal*, *90*, 511–518. https://doi.org/10.2134/agronj1998.00021962009000040012x

Sainju, U. M., Whitehead, W. F., & Singh, B. P. (2003). Cover crops and nitrogen fertilization effects on soil aggregation and carbon and nitrogen pools. *Canadian Journal of Soil Science*, *83*, 155–165. https://doi.org/10.4141/S02-056

Schulte, L. A., Niemi, J., Helmers, M. J., Liebman, M., Arbuckle, J. G., James, D. E., … Witte, C. (2017). Prairie strips improve biodiversity and the delivery of multiple ecosystem services from corn–soybean croplands. *Proceedings of the National Academy of Sciences of the United States of America*, *114*, 11247–11252. https://doi.org/10.1073/pnas.1620229114

Sonderegger, D. (2011). SiZer: Significant zero crossings. R package version 0.1-5. Retrieved from https://cran.r-project.org/web/packages/SiZer/index.html

Stenberg, B., Johansson, M., Pell, M., Sjödahl-Svensson, K., Stenström, J., & Torstensson, L. (1998). Microbial biomass and activities in soil as affected by frozen and cold storage. *Soil Biology and Biochemistry*, *30*, 393–402. https://doi.org/10.1016/S0038-0717(97)00125-9

Thapa, R., Mirsky, S. B., & Tully, K. L. (2018). Cover crops reduce nitrate leaching in agroecosystems: A global meta-analysis. *Journal of Environmental Quality*, *47*, 1400–1411. https://doi.org/10.2134/jeq2018.03.0107

Tiemann, L. K., & Grandy, A. S. (2015). Mechanisms of soil carbon accrual and storage in bioenergy cropping systems. *Global Change Biology – Bioenergy*, *7*, 161–174. https://doi.org/10.1111/gcbb.12126

von Lützow, M., Kögel-Knabner, I., Ekschmitt, K., Flessa, H., Guggenberger, G., Matzner, E., & Marschner, B. (2007). SOM fractionation methods: Relevance to functional pools and to stabilization mechanisms. *Soil Biology and Biochemistry*, *39*, 2183–2207. https://doi.org/10.1016/j.soilbio.2007.03.007

Wang, Y., Cerling, T. E., & Effland, W. R. (1993). Stable isotope ratios of soil carbonate and soil organic matter as indicators of forest invasion of prairie near Ames, Iowa. *Oecologia*, *95*, 365–369. https://doi.org/10.1007/BF00320990

Wedin, D. A., & Tilman, D. (1996). Influence of nitrogen loading and species composition on the carbon balance of grasslands. *Science*, *274*, 1720–1723. https://doi.org/10.1126/science.274.5293.1720

Wynn, J. G., & Bird, M. I. (2007). C_4-derived soil organic carbon decomposes faster than its C_3 counterpart in mixed C_3/C_4 soils. *Global Change Biology*, *13*, 2206–2217. https://doi.org/10.1111/j.1365-2486.2007.01435.x

Yue, K., Peng, Y., Peng, C., Yang, W., Peng, X., & Wu, F. (2016). Stimulation of terrestrial ecosystem carbon storage by nitrogen addition: A meta-analysis. *Scientific Reports*, *6*, 19895. https://doi.org/10.1038/srep19895

Zan, C. S., Fyles, J. W., Girouard, P., & Samson, R. A. (2001). Carbon sequestration in perennial bioenergy, annual corn and uncultivated systems in southern Quebec. *Agriculture, Ecosystems & Environment*, *86*, 135–144. https://doi.org/10.1016/S0167-8809(00)00273-5

Zimmermann, M., Leifeld, J., Schmidt, M. W. I., Smith, P., & Fuhrer, J. (2007). Measured soil organic matter fractions can be related to pools in the RothC model. *European Journal of Soil Science*, *58*, 658–667. https://doi.org/10.1111/j.1365-2389.2006.00855.x

SUPPORTING INFORMATION

Additional supporting information may be found online in the Supporting Information section.

How to cite this article: Ye C, Hall SJ. Mechanisms underlying limited soil carbon gains in perennial and cover-cropped bioenergy systems revealed by stable isotopes. *GCB Bioenergy*. 2019;00:1–17. https://doi.org/10.1111/gcbb.12657